Alkali corrosion resistant coatings for Si_3N_4 ceramics

T. K. LI, D. A. HIRSCHFELD, J. J. BROWN
Materials Science and Engineering Department, Virginia Polytechnic Institute and State University, Blacksburg, Virginia 24061-0256, USA

The use of ceramic oxide coatings on silicon nitride is one method to improve its alkali corrosion resistance. Four oxide coatings, including $(Ca_{0.6}, Mg_{0.4})\ Zr_4(PO_4)_6$ (CMZP), zirconia, mullite and alumina, were examined. These coatings were applied on Si_3N_4 using both sol–gel and dip coating techniques. The coated and uncoated samples were exposed to sodium molten-salt and sodium-containing atmospheres at 1000 °C for 50 h. The weight loss of all the coated samples was less than that of the uncoated Si_3N_4 with CMZP-coated samples exhibiting the smallest weight loss. There was no decrease in the flexural strength of Si_3N_4 after coating with zirconia and CMZP, and a decrease in strength after coating with either mullite or alumina. After alkali exposure, the strength of the CMZP and zirconia coated samples were significantly higher than those of the mullite-coated, alumina-coated, and uncoated Si_3N_4. The observed behaviour is explained in terms of the microstructure and protection mechanisms.

1. Introduction

Ceramics in general are known for their thermal stability, and often exhibit excellent resistance to wear and corrosion, as well. Therefore, a great number of ceramic materials are candidates for applications in high-temperature, extremely corrosive environments encountered in a wide range of industries. Particularly challenging to the reliability of structural ceramic components are those applications requiring good resistance to attack by alkalis. These applications include: (a) refractories subjected to the action of alkali vapours or slag in glass furnaces, blast furnaces and stove construction, cement kiln linings, combustion chamber boilers and town gas installations [1–4]; (b) advanced high temperature coal conversion and combustion, heat exchangers, and other energy systems [5–9]. But it was found that many ceramics can be attacked rapidly by alkali; therefore, the protection of ceramics from alkali corrosion is an important subject.

Currently, many materials in high temperature service are performing at their capability limits. As material requirements become increasingly sophisticated, it is becoming more and more difficult to combine the required structural properties and stability in a single material. The application of high temperature corrosion resistant material to substrates which possess the required mechanical properties for a specific application can produce cost-effective composite systems which optimize both corrosion resistance and strength.

Since non-oxide ceramics such as silicon nitride show outstanding fracture strength at high temperatures and excellent thermal shock resistance, they can be fabricated into required shapes and sizes, and they are good candidates for structure applications at high temperature. However, silicon nitride corroded severely in atmospheres containing alkali compounds. In contrast, certain oxide ceramic materials, such as alumina, mullite, zirconia and CMZP, exhibit superior corrosion resistance to alkali [2, 3, 10, 11]. Thus, ceramic oxide coatings may be applied to Si_3N_4 combining the superior thermo-mechanical properties of Si_3N_4 with the corrosion resistance of the oxide ceramics.

Silicon nitride is thermodynamically unstable in air and relies on a thin film of SiO_2 for oxidation protection. Alkali attacks Si_3N_4 and is a process of oxidation corrosion by dissolving the SiO_2 protective film [7]. According to the corrosion mechanism of Si_3N_4 ceramics, to prevent corrosion, the refractory nature of the SiO_2 film should be retained as much as possible, which could be accomplished by introducing another compound into the film. The compound could be applied as a coating on the Si_3N_4 substrate specifically to react with the SiO_2 film and alkali to produce a more refractory layer. Some possible coating materials are Al_2O_3, Cr_2O_3, MgO, TiO_2, ZrO_2 etc. [12]. They might assist in maintaining a solid reaction layer or at least minimize corrosion of the Si_3N_4 ceramics according to their respective phase diagram. Many coating technologies can be used to prepare a protective layer of ceramics on a substrate. The advantages of using sol–gel techniques for coatings is well known and include achieving oxygen and ionic stoichiometry during the formation reactions. Atomic association in

0022–2461

a solution leads to a lower crystallographic formation energy, and forms single phase materials having complex compositions. Since the chemical reactants for sol–gel processing can be purified conveniently by distillation and crystallization, a coating of high purity can be fabricated by sol–gel processing. Another benefit is the ability to coat complex shapes, including parts having blind holes and corners, long tapes and wires, curved surfaces, and the inside surfaces of cylinders. Also, coating adhesion is excellent [13–15].

The present work focuses on the alkali corrosion and protective mechanism of Si_3N_4 ceramics coated by oxide materials. The sol–gel coating techniques were developed for application of the corrosion-resistant coatings. The corrosion behaviour of coating materials in alkali molten-salt, and alkali-containing atmospheres was evaluated. The effect of the alkali molten-salt, and alkali-containing atmospheres upon coating characteristics such as microstructure, interface adhesion, chemical composition of the surface, weight changes, strength of coated and uncoated samples, was examined.

2. Experimental procedure

2.1. Materials

A single batch of commercially available Si_3N_4 with 6 wt % Y_2O_3 (PY-6) as a sintering aid was used in this study. Samples used for the measurement of corrosion rate and strength degradation were cut into rectangular coupons, 2 mm by 3 mm by 10 mm and 2 mm by 3 mm by 50 mm, respectively.

In order to prepare crack-free coatings and enhance the adhesion of the coatings to Si_3N_4 substrate, the carrier surface was treated to form an oxide layer. First the silicon nitride samples were washed with acetone, dried at 110 °C for 2 h, then immersed in 20% HF for 10 min. Finally, the samples were washed with deionized water, and calcined at 1200 °C for 6 h.

2.2. Preparation of solutions for coatings

The basic principle of the sol–gel process is to form a solution of the elements of the desired compound in an organic solvent, polymerize the solution to form a gel, then dry and fire this gel to displace the organic components to form a final oxide.

2.2.1. CMZP solution

First the precursors, $Ca(CH_3CO_2)_2H_2O$, $Mg(C_2H_5O)_2$, $Zr(C_2H_5O)_4$, and $(C_2H_5O)_3P(O)$, were mixed in stoichiometric proportions in ethyl alcohol or deionized water. Then the mixture was slowly stirred while HCl was added dropwise until pH 2 was reached. A clear CMZP solution was formed.

2.2.2. Zirconia solution

The precursors, $Zr(C_2H_5O)_4$ and $YCl \cdot 6H_2O$, were mixed in stoichiometric proportions in ethyl alcohol, then were kept at 90 °C and stirred while 1 mol water, and 0.1 mol HCl per mol of $Zr(C_2H_5O)_4$ was added. The solution was kept boiling until a clear solution was formed.

2.2.3. Alumina solution

The precursor was $((CH_3)_2CHO)_3Al$. First aluminium isopropoxide was added to deionized water which was heated to about 90 °C while vigorously stirring. The solution was kept at 90 °C for 2 h, then 0.07 mol HCl per mol alkoxide was added to peptize the sol particles. The sol was kept boiling in an open reactor until a clear solution was formed.

2.2.4. Mullite solution

The precursor were $((CH_3)_2CHO)_3Al$ and $Si(OC_2H_5)_4$. First aluminium isopropoxide was added to deionized water which was heated to about 90 °C while vigorously stirring. The solution was kept at 90 °C for 2 h, then $Si(OC_2H_5)_4$ was added. Finally, 0.07 mol HCl per mol alkoxide was added to peptize the sol particles. The sol was kept boiling in an open reactor until a clear solution was formed.

2.3. Coating techniques

CMZP, zirconia, alumina and mullite coatings on silicon nitride substrate were prepared by sol–gel and dip techniques. The procedures are described schematically in Fig. 1. First, the ceramic samples were immersed in the solutions for 5 min, and were taken out of the solutions at a rate of 4–12 cm min^{-1} by the dip machine. The coated samples were kept at room temperature for 4 days, and dried at 40–60 °C for 2 days to form clear gel coatings. After the drying process, the samples coated by CMZP were fired at 1200 °C for 24 h, while the samples coated by zirconia, alumina or mullite were fired at 1500 °C for 10 h. The heating schedule consisted of a heating rate of 0.5 °C min^{-1} from room temperature to 500 °C; holding 2 h at 200, 300, 400 and 500 °C, respectively; rapid heating from 500 to 1500 °C at a rate of 5 °C min^{-1}, and 4 h hold at 1000 °C and 10–24 h hold at 1200–1500 °C.

2.4. Thermal shock test

Five coated Si_3N_4 samples for each coating and each test, approximately 2 mm by 3 mm by 10 mm, were tested for thermal shock resistance. The samples were heated to 300, 500 and 1000 °C, respectively, and then quenched in water at 25 °C. The surface microstructure of coatings and adhesion between the coatings and Si_3N_4 substrate were examined by scanning electron microscopy (SEM).

2.5. Alkali corrosion test

The alkali corrosion resistance of both coated and uncoated Si_3N_4 ceramics was examined by determining the weight loss and strength degradation of samples exposed to Na_2CO_3 molten-salt and sodium-containing atmospheres at 1000 °C for 50 h. Five

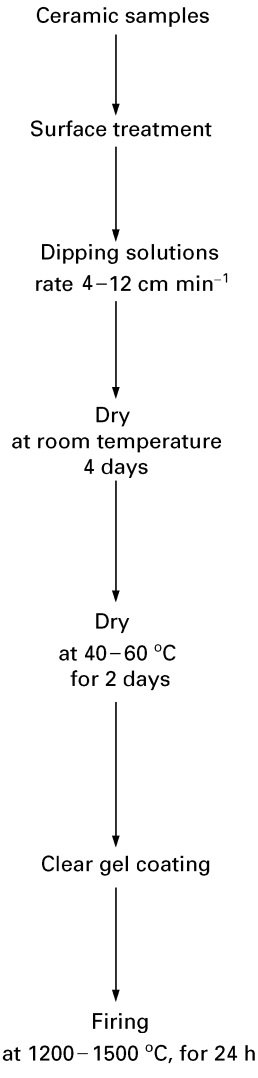

Figure 1 The coating process for Si_3N_4 substrates.

samples for each coating and each corrosion test were used in this study.

Weighted samples were heated to 200 °C, then dipped into a saturated solution of Na_2CO_3. The quantity of salt adhering to the samples was determined by weighing after suitable drying, and controlled to 2–3 mg cm^{-2}.

Two corrosion conditions were used in this study. (i) The sodium-coated samples were placed in an electric furnace regulated at 1000 °C for 50 h. (ii) The sodium-coated samples were exposed to a sodium-containing atmosphere at 1000 °C for 50 h. To determine the weight loss after the exposure, the samples were washed in distilled water at 100 °C to remove any residual salt and sodium silicates, then chemically etched in 10% HF acid to remove the surface corrosion products prior to weighing. Etching was performed until no noticeable difference in weight change with time was recorded. The room-temperature flexure strength of both as-received and corroded Si_3N_4 samples were determined by four-point bending using a ATS model 1120 universal test machine. The bend test had an outer span of 40 mm and inner span of 20 mm and a loading rate of 0.05 cm min^{-1} (0.02 in min^{-1}).

The microstructure and fracture surfaces of the samples both before and after corrosion were examined by SEM with energy dispersive X-ray analysis (EDX) (Phillips model PW 1840). Also, the phases of sample surfaces before and after corrosion were identified using the standard X-ray diffraction (XRD) technique (International Scientific Instrument, model SX-40 and EDX equipment).

3. Results and discussion

3.1. Coatings

The microstructure of CMZP, zirconia, alumina and mullite coatings on Si_3N_4 substrates is described on Table I and shown in Fig. 2. The phase identification of the coatings is shown in Table II. For CMZP and zirconia coatings, the oxidation layer on the Si_3N_4 samples by the surface treatment improved the coating adhesion and resulted in dense thin film coating. Homogeneous, crack-free coatings were formed on the surface of the silicon nitride samples with excellent interfacial bonding. The CMZP coating thickness, ranging from 1 to 4 μm, was found to vary with concentration in the coating solution. Fig. 2 shows the surface microstructure of CMZP and zirconia coatings and interface between the coating and the silicon nitride substrate. The grains exhibited a uniform grain size of about 2–3 μm. The phase identification showed that the CMZP coating was primary single phase, and the zirconia coating consisted of tetragonal zirconia (t-ZrO_2) and zircon resulting from the reaction between the zirconia and the silicon on the surface of the Si_3N_4 substrate.

For the alumina and mullite coatings on the Si_3N_4 substrate, SEM and phase identification by X-ray indicated formation of an aluminosilicate glass layer with some bubbles on the surface of the Si_3N_4 (Fig. 2). It was suggested that the presence of alumina with silica at concentrations below that required for stoichiometric mullite, or existence of impurities may result in the creation of either a metastable eutectic, as reported by Aksay and Pask [16], to be around 1250 °C, or immiscible aluminosilicate liquids, as reported by MacDowel and Beals [17], and enhancing the oxidation of Si_3N_4 accomplished by the formation of N_2 which results in the defects on the surface of Si_3N_4. Borow *et al.* [18] also found that the existence of alumina or mullite can enhance the oxidation of silicon carbide. This is consistent with the above analysis. Because of the surface defects and reaction, the strength of Si_3N_4 samples coated with either alumina or mullite decreased before alkali corrosion as shown on Table III.

The thermal shock results of coated Si_3N_4 are shown in Table IV and Fig. 3. CMZP coatings have good thermal shock resistance because of the low thermal expansion mismatch and excellent adhesion to the Si_3N_4 substrate. The SEM micrograph (Fig. 3) of the surface microstructure of the CMZP coating after the 1000 °C thermal shock test shows that even though a crack is formed, there is no spalling. The alumina and mullite coatings also exhibit good thermal shock resistance with only a few small cracks

TABLE I The characteristics of coatings on Si_3N_4

	Coatings			
	CMZP	ZrO_2	Al_2O_3	$3Al_2O_32SiO_2$
Precursors	organic	organic	organic	organic
Surface	uneven	flat	flat with bubbles	flat with bubbles
Grain size (μm)	2–3	2–3	–	–
Morphology of grains	hexahedron	spheroid	glass phase	glass phase
Thickness of coatings (μm)	1–4	2–3	2–3	2–4
Coating adhesion	excellent	excellent	excellent	excellent

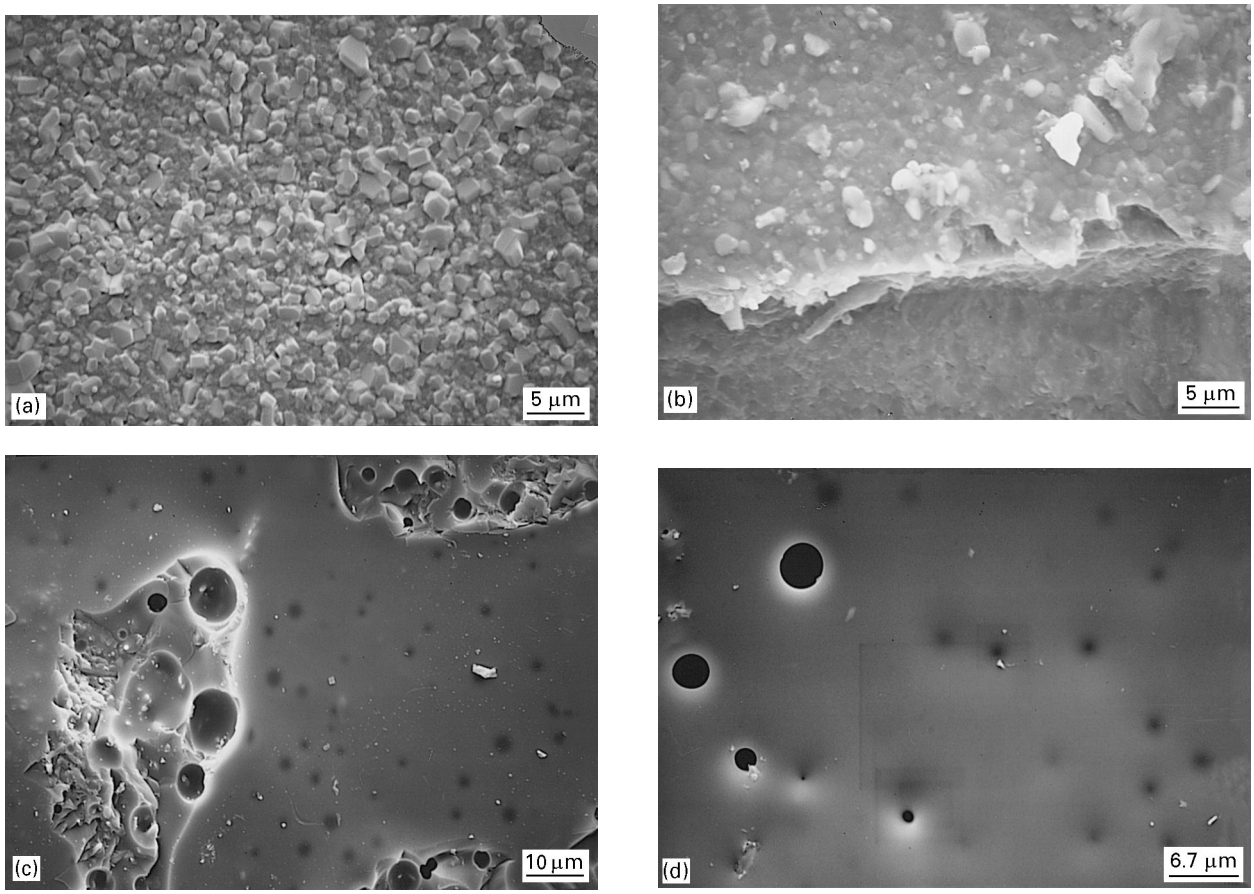

Figure 2 (a) The surface microstructure of the CMZP coating. (b) The surface microstructure of the ZrO_2 coating. (c) The surface microstructure of the Al_2O_3 coating. (d) The surface microstructure of $3Al_2O_3 \cdot 2SiO_2$ coating.

TABLE II Phase identification of coatings

	Before corrosion	Na_2CO_3 molten-salt at 1000 °C, 50 h	Na_2CO_3 molten-salt + vapour at 1000 °C, 50 h
CMZP	CMZP	CMZP	CMZP + amorphous
ZrO_2	t-ZrO_2 + zircon	t-ZrO_2 + zircon	m-ZrO_2 + zircon
Al_2O_3	amorphous	amorphous	amorphous
Mullite	amorphous	amorphous	amorphous

forming after 1000 °C thermal shock. Compared with other coatings, the zirconia coating exhibits poor thermal shock resistance. Due to a larger mismatch of the coefficient of thermal expansion (CTE) between the zirconia coating and the Si_3N_4 substrate, CTE of zircon is $4\times10^{-6}\,°C^{-1}$, CTE of t-ZrO_2 is $9.4\times10^{-6}\,°C^{-1}$, and CTE of Si_3N_4 is $3\times10^{-6}\,°C^{-1}$. In zirconia coating, cracks formed after the 500 °C thermal shock test while both cracks and spallings occurred following the 1000 °C thermal shock test.

3.2. Alkali corrosion of silicon nitride

The sodium corrosion of Si_3N_4 samples is shown on Table III. Compared to Si_3N_4 coated with CMZP or zirconia, uncoated Si_3N_4 exhibits a greater weight loss

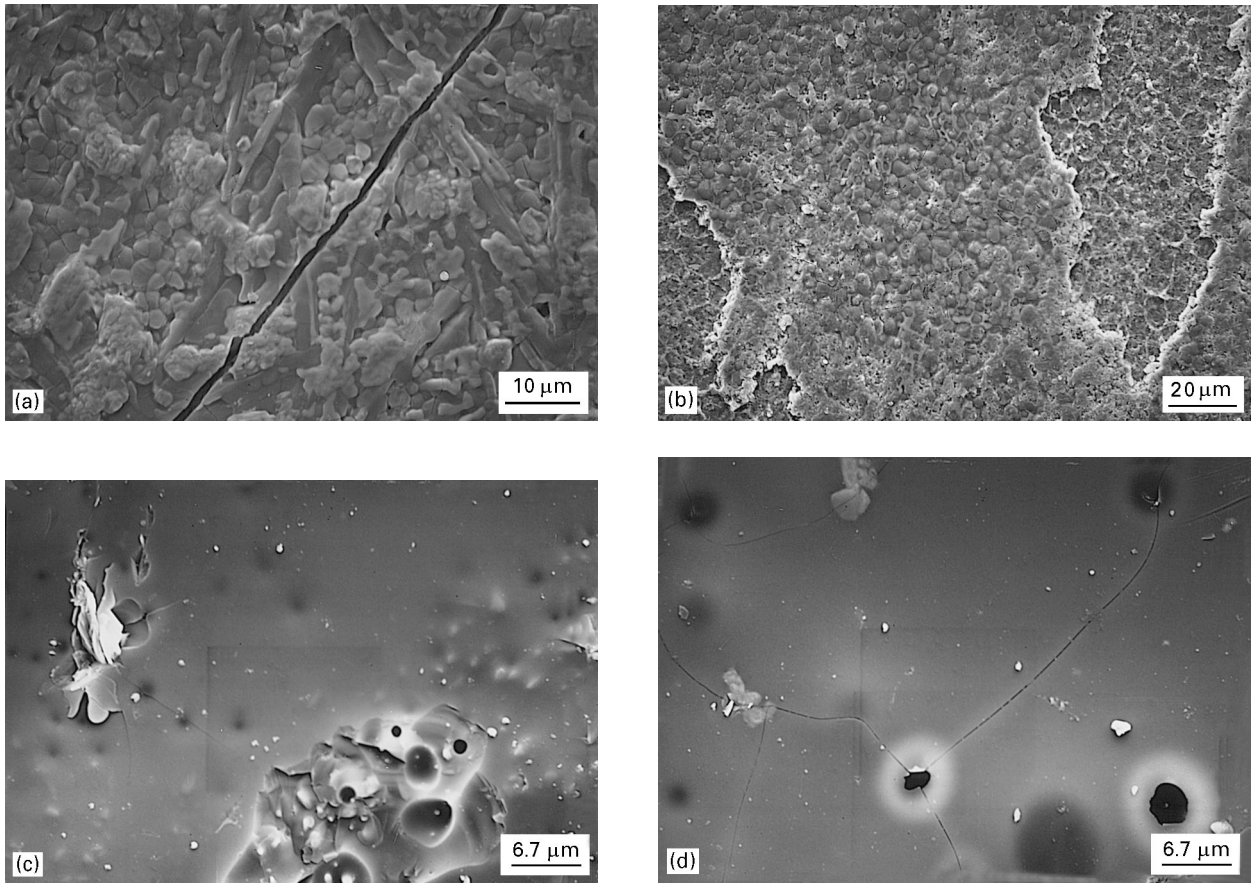

Figure 3 (a) The microstructure of the CMZP coating after 1000 °C thermal shock. (b) The microstructure of the ZrO_2 coating after 1000 °C thermal shock. (c) The microstructure of the Al_2O_3 coating after 1000 °C thermal shock. (d) The microstructure of the $3Al_2O_3{\cdot}2SiO_2$ coating after 100 °C thermal shock.

TABLE III Alkali corrosion resistance of coatings

	Before corrosion	Na_2CO_3 molten-salt at 1000 °C, 50 h		Na_2CO_3 molten-salt + vapour at 1000 °C, 50 h	
	Strength (MPA)	Weight loss (%)	Strength (MPa)	Weight loss (%)	Strength (MPa)
CMZP	593 + 11	1.68 + 0.3	669 + 11	5.24 + 0.5	611 + 12
ZrO_2	583 + 17	3.16 + 0.1	763 + 18	6.77 + 0.7	721 + 27
Al_2O_3	363 + 21	3.00 + 0.2	462 + 12	4.11 + 0.5	507 + 16
Mullite	403 + 19	2.51 + 0.7	408 + 8	4.04 + 0.3	485 + 8
Si_3N_4	595 + 10	4.41 + 0.2	573 + 8	7.04 + 0.2	546 + 12

TABLE IV Thermal shock resistance of coatings on Si_3N_4

Coatings	300 °C	500 °C	1000 °C
CMZP	no crack	no crack	cracks
ZrO_2	no crack	small cracks	crack and spalling
Al_2O_3	no crack	no crack	small cracks
Mullite	no crack	no crack	small cracks

and reduction in strength. Scanning electron micrographs show the limited depth of penetration of the corrosion into the silicon nitride and the existence of holes at the surface (Fig. 4).

Silicon nitride is thermodynamically unstable in air and relies on a thin film of SiO_2 for oxidation protection. The SiO_2 film on Si_3N_4, although very thin, is normally protective in an oxidizing atmosphere at 1200 °C. The presence of sodium with Si_3N_4 dissolves the SiO_2 protective film and enhances oxidation.

Based on thermogravimetric analyses and morphology observations on Si_3N_4 after corrosion by Na_2CO_3, it is suggested that the following reaction mechanisms occur: (i) decomposition of Na_2CO_3 and formation of Na_2SiO_3, (ii) rapid oxidation, (iii) formation of a protective silica layer below the silicate and a slowing of the reaction, and (iv) the protective silica layer is corroded further. The reaction formulae follow [7]:

$$SiO_2(s) + Na_2O(s) = Na_2SiO_3(s) \quad (1)$$

$$Si_3N_4(s) + 3O_2(g) = 3SiO_2(s) + 2N_2(g) \quad (2)$$

The protective SiO_2 film is dissolved to form Na_2SiO_3. Accelerated scale growth occurs because the silicate is liquid at 1000 °C. Gas evolution (N_2)

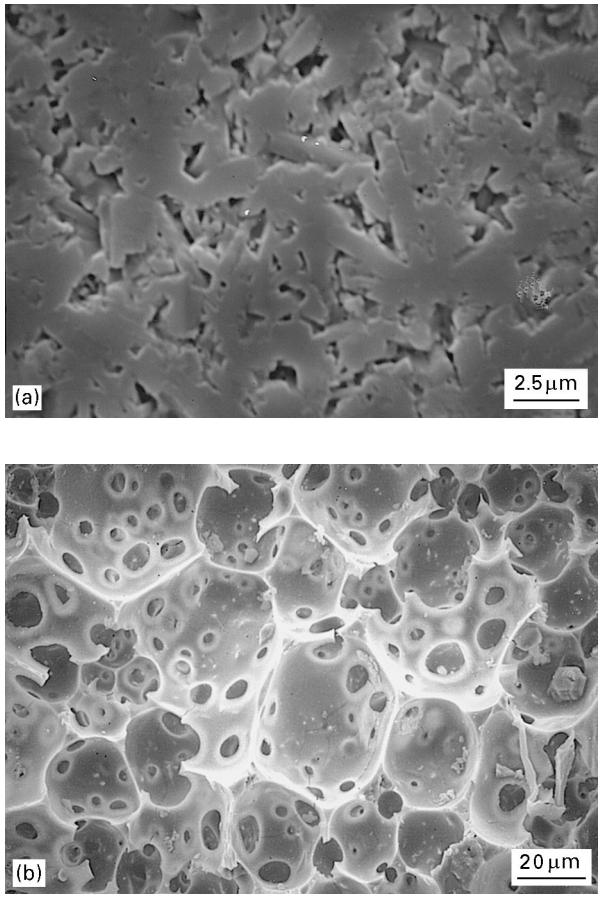

Figure 4 (a) The surface of Si_3N_4 before sodium corrosion. (b) The surface of Si_3N_4 after sodium corrosion.

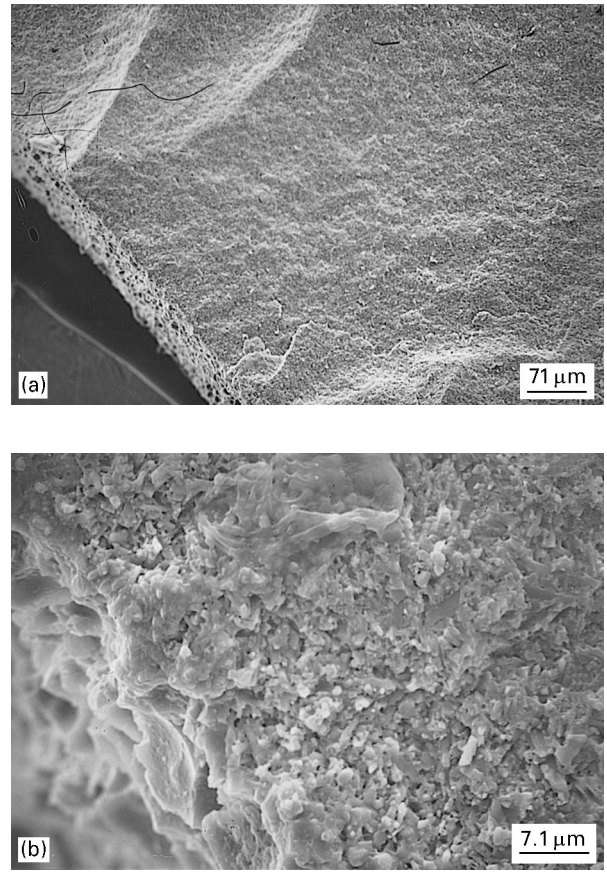

Figure 5 (a) The fracture origin region of Si_3N_4 after sodium corrosion. (b) The fracture origin: surface defects.

accounts for the formation of bubbles in the glassy scale. Extensive pitting causes strength reduction.

Because the fabrication of dense silicon nitride requires additives such as Y_2O_3, preferential attack of the grain boundary phase occurred. Chemical attack of the grain boundaries formed pits which enhanced crack growth, and resulted in a strength reduction for the Si_3N_4 materials [7, 19, 20], as observed in these experimental results. The analysis of fracture origin also confirmed further that the surface defects caused by sodium corrosion resulted in fracture of the uncoated Si_3N_4 samples (Fig. 5).

3.3. Alkali corrosion resistance of coatings

The alkali corrosion resistance of Si_3N_4 substrates coated by CMZP, zirconia, alumina, and mullite are shown in Table III. The weight loss of all the coated samples was less than that of the uncoated Si_3N_4 with CMZP-coated samples exhibiting the smallest weight loss. No decrease in the flexural strength of the Si_3N_4 samples after coating with CMZP and zirconia was observed (Table III). It may be because of formation of the dense CMZP and zirconia coatings on the Si_3N_4 substrate. After sodium exposure, the strength of the CMZP-coated samples were significantly higher than that of the uncoated silicon nitride. According to the corrosion mechanism of Si_3N_4 ceramics, alkali enhanced oxidation of the ceramics occurs by dissolving the protective SiO_2 layer. To prevent this corrosion, the refractory nature of the SiO_2 film should be retained as much as possible, which could be accomplished by introducing another compound into the film. Therefore, it is suggested that the CMZP reacts with the SiO_2 film on the surface of the Si_3N_4 substrate and sodium to produce a more refractory layer, which assists in maintaining a continuous reaction layer and minimizes corrosion. The SEM micrograph showed that a dense protective layer on the surface of Si_3N_4 coated by CMZP is formed after sodium corrosion (Fig. 6). With increasing sodium concentration, the melting point of the protective layer decreased, so that corrosion occurred further (Fig. 7).

Zirconia also formed a dense coating on the surface of Si_3N_4 with an intermediate layer of zircon between the zirconia and the Si_3N_4. Because zirconia exhibits good alkali corrosion resistance [21], the Si_3N_4 samples coated by zirconia had less weight loss and higher strength than that of uncoated Si_3N_4 samples (Table III). However, the stabilizing additives have less alkali corrosion resistance than zirconia [22], with increasing sodium concentration, the sodium leaching of the stabilizer from the zirconia leads to a transformation from tetragonal to monoclinic zirconia as shown on Table II, which caused cracks to form in the coating, resulting in further corrosion along with the cracks (Fig. 8). It has been reported that scandia-stabilized zirconia is superior to yttria-stabilized zirconia in resistance to alkali corrosion, followed by MgO- and CaO-stabilized zirconia [23, 24]. Therefore, the use of scandia as a stabilizer may improve alkali corrosion resistance of zirconia coating.

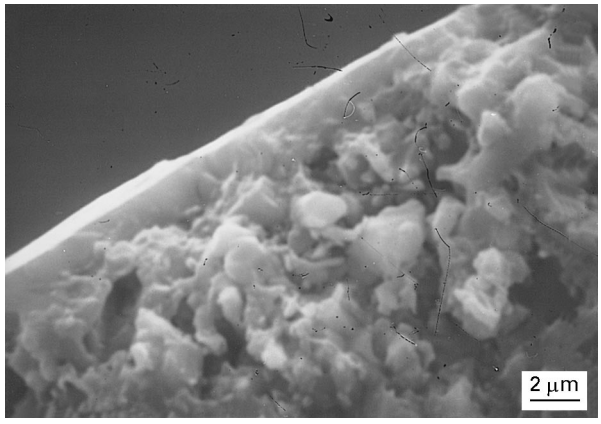

Figure 6 The formation of the dense protective layer on the surface of Si_3N_4 coated by CMZP after sodium corrosion.

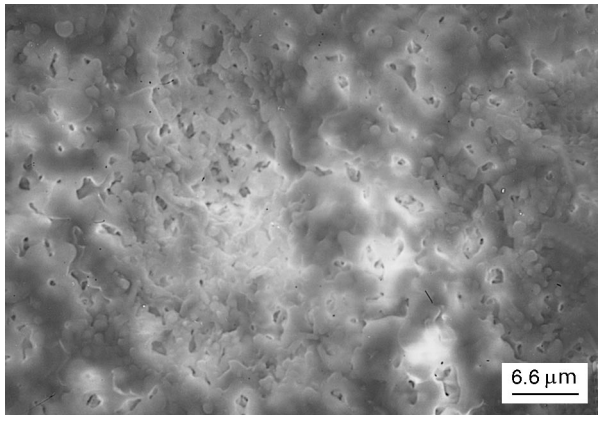

Figure 7 The corrosion surface of the CMZP coating after exposure to both molten-salt and vapour of sodium carbonate.

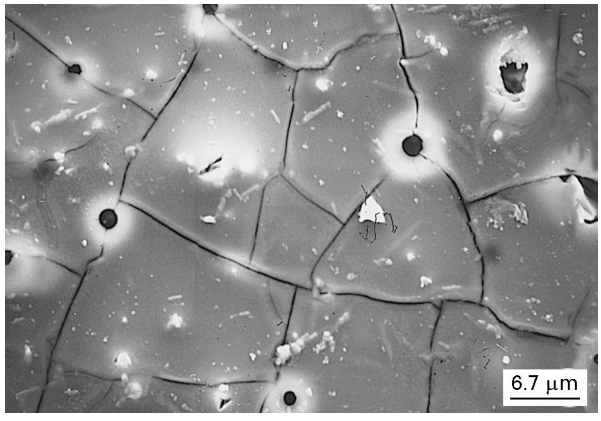

Figure 8 The corrosion surface of the ZrO_2 coating after exposure to both molten-salt and vapour of sodium carbonate.

Amorphous aluminosilicate films were formed on the surface of the Si_3N_4 substrate coated with alumina and mullite. Compared with Si_3N_4, the aluminosilicate has higher alkali corrosion resistance, as evidenced by a weight loss less than that of uncoated Si_3N_4, and almost no degradation in strength after sodium corrosion (Table III). However, because the strength of Si_3N_4 was decreased after coating with either alumina or mullite prior to alkali exposure, the application of alumina and mullite as a protective coating on Si_3N_4 substrate may be limited.

4. Conclusion

Ceramic oxide coatings on silicon nitride, including $(Ca_{0.6}, Mg_{0.4})Zr_4(PO_4)_6$ (CMZP), zirconia, mullite and alumina, were shown to improve its alkali corrosion resistance. CMZP and zirconia coatings improve the alkali corrosion of Si_3N_4 as evidenced by less weight loss and higher flexure strength after corrosion.

Alumina and mullite coatings also improve the alkali corrosion resistance of Si_3N_4, but due to observable degradation in strength of the Si_3N_4 samples after coating with either alumina or mullite prior to alkali corrosion, their application is limited.

Acknowledgements

This work was sponsored by the US Department of Energy, Ceramic Technology for Advanced Heat Engines Project through subcontract with Martin Marietta Energy Systems No. 86X22049C, and the Virginia CIT Center for Advanced Ceramic Materials.

References

1. R. E. FARRIS and J. E. ALLEN, *Iron Steel Engng* **2** (1973) 67.
2. M. V. ROODE, J. R. PRICE, R. R. GILDERSLEEVE and C. E. SMELTZER, *Ceram. Engng Sci. Proc.* **9** (1988) 1245.
3. J. R. ORICE and M. V. ROODE, *Ceram. Trans.* **10** (1990) 469.
4. G. R. RIGBY and R. HUTTON, *J. Amer. Ceram. Soc.* **45** (1962) 68.
5. N. S. JACOBSON and J. L. SMIALEK, *ibid.* **68** (1985) 432.
6. J. SAWYER, R. J. VASS, N. R. BROWN and J. J. BROWN, *Trans. ASME*, **90-GT-347** (1991).
7. D. S. FOX and N. S. JACOBSON, *J. Amer. Ceram. Soc.* **71** (1988) 128.
8. N. S. JACOBSON and D. S. FOX, *ibid.* **71** (1988) 139.
9. T. SATO, K. KUBOTA and M. SHIMADA, *ibid.* **74** (1991) 2152.
10. L. M. SHEPPARD, *Ceram. Bull.* **70** (1991) 1146.
11. T. K. LI, D. A. HIRSCHFELD and J. J. BROWN, *J. Mater. Res. Soc.* **9** (1994) 2014.
12. J. I. FEDERER, *Adv. Ceram. Mater.* **3** (1988) 56.
13. L. C. KLEIN and N. GISZPENC, *Amer. Ceram. Soc. Bull.* **69** (1990) 1821.
14. H. G. FLOCH and J. J. PRIOTTON, *ibid.* **69** (1990) 1141.
15. G. YI and M. SAYER, *ibid.* **70** (1991) 1173.
16. A. AKASY and J. A. PASK, *J. Amer. Ceram. Soc.* **58** (1975) 507.
17. J. F. MACDOWEL and G. M. BEALS, *ibid.* **52** (1969) 17.
18. M. P. BOROW, M. K. BRUN and L. E. SZALA, *Adv. Ceram. Mater.* **3** (1988) 491.
19. C. H. HENAGER Jr and R. H. JONES, *Ceram. Trans.* **10** (1990) 197.
20. D. S. FOX and J. L. SMIALEK, *J. Amer. Ceram. Soc.* **73** (1990) 303.
21. G. R. PICKRELL, T. SUN and J. J. BROWN, Quarterly Progress Report 4 for the period 1 June–31 August (The Center for Advanced Ceramic Materials, Virginia Tech., Blacksburg, VA 24061, 1992).
22. R. L. JONES, C. E. WILLIAMS and S. R. JONES, *J. Electrochem. Soc.* **133** (1986) 227.
23. K. E. MORI, T. N. FULMO *et al. Yogyo Kyokaishi.* **95** (1987) 595.
24. R. L. JONES, *High Temp. Sci.* **27** (1987) 3629.

Received 18 October 1995
and accepted 10 February 1997